IEEE Access
Multidisciplinary | Rapid Review | Open Access Journal

SPECIAL SECTION ON ADVANCES IN INTERFERENCE MITIGATION TECHNIQUES FOR DEVICE-TO-DEVICE COMMUNICATIONS

Received December 2, 2017, accepted January 23, 2018, date of publication January 30, 2018, date of current version March 12, 2018.

Digital Object Identifier 10.1109/ACCESS.2018.2799626

Large System Analysis of Heterogeneous Cellular Networks With Interference Alignment

XUE JIANG[1,2], BAOYU ZHENG[1], (Senior Member, IEEE), WEI-PING ZHU[1,3], (Senior Member, IEEE), LEI WANG[1,2], (Member, IEEE), AND YULONG ZOU[1], (Senior Member, IEEE)

[1]School of Communication and Information Engineering, Nanjing University of Posts and Telecommunications, Nanjing 210003, China
[2]State Key Laboratory of Integrated Services Networks, Xidian University, Xi'an 710000,China
[3]Department of Electrical and Computer Engineering, Concordia University, Montreal QC H3G 1M8, Canada

Corresponding author: Xue Jiang (jiangx@njupt.edu.cn)

This work was supported in part by the National Science Foundation of China under Grant 61671253, Grant 61401223 and Grant 61522109, in part by the Major Projects of the Natural Science Foundation of the Jiangsu Higher Education Institutions under Grant 16KJA510004, in part by the Open Research Fund of The State Key Laboratory of Integrated Services Networks, Xidian University under Grant ISN17-04, in part by the Open Research Fund of National Mobile Communications Research Laboratory, Southeast University under Grant 2016D01, in part by the Open Research Fund of Key Lab of Broadband Wireless Communication and Sensor Network Technology (NUPT), Ministry of Education of china under Grant NYKL201509, in part by the Natural Science Foundation of Jiangsu Province under Grant BK20150040 and Grant BK20171446, and in part by the Key Project of Natural Science Research of Higher Education Institutions of Jiangsu Province under Grant 15KJA510003.

ABSTRACT In this paper, we conduct large system analysis of heterogeneous cellular networks (HCNs) which are modeled as a two-tier cellular network consisting of one macro base station (MaBS) and multiple micro base stations (MiBSs) distributed according to a Poisson point process. Interference alignment is performed via rank constrained rank minimization (RCRM) to design the transmit precoding and receive beamforming matrices of the users in HCNs for the suppression of interference signal. We then analyse the average achievable rate for both macro users (MaUEs) and micro users (MiUEs) with an objective of obtaining a closed-form expression. It is shown that the MaUE and MiUE rate expressions are functions of the transmit power, noise power, MiBS density, and the transmit distance. Extensive simulations show that the rate expressions derived through large system analysis provide accurate estimates of the average achievable rates of HCNs with different system parameters.

INDEX TERMS Heterogeneous cellular networks (HCNs), interference alignment, large system analysis, random matrix theory, stochastic geometry, rank constrained rank minimization.

I. INTRODUCTION

IN the future fifth generation (5G) communication systems, the architecture of network will transform from traditional cellular networks to heterogeneous cellular networks (HCNs) [1], [2]. A HCN shall consist of conventional macro cellular networks overlaid with an irregular deployment of low-power base stations (BSs), serving small cells and shall offer a significant capacity gain. To achieve this capacity gain, however, the interference should be carefully handled. Interference alignment [3]–[9] is one of the techniques that have been proposed to manage the interference in homogeneous cellular networks, which is different from traditional interference processing approaches. Specifically, it uses spatial beam-forming to divide a signal space into the desired signal subspace and the interference subspace at the receiver by multiple antennas. If all the interference can be aligned into an interference subspace, they will not extend to the desired signal space, so that the desired signal does not fall into the interference subspace, and thus the receiver can easily attain its desired signal. Paper [10] proposed a novel scheme in IA wireless networks, showing that interference alignment is one of the key issues in next generation wireless systems. Many studies have been focused on interference alignment in HCNs. In co-channel heterogeneous cellular networks [11], the multiuser interference subspace is aligned with the partial inter-cell interference subspace and suppressed at the receiver. SarahImam and El-Mahdy [12] proposed a cross-tier interference alignment algorithm for

5G cellular wireless networks. Paper [13] proposed an interference alignment based transmit precoding scheme with different user selection methods in a heterogeneous network.

As one of the most important system performance metrics for heterogeneous cellular networks, analysis of users' rate has attracted much attention for long time, but it is very difficult to obtain the expressions of the achievable rates in a closed-form. This is mainly due to the complicated channel characteristics which are affected by several factors including: the number of users, the number of receivers, and the number of transmit and receive antennas. Large system analysis (LSA) [14]–[18] is shown to be a very useful tool for computing the achievable rates as the rate expressions obtained through LSA usually provide a very good estimate for systems. LSA is performed by fixing the number of users and letting the number of transmitting and receiving antennas approach infinity at a finite fixed ratio. It is revealed that the eigenvalue or singular value distributions of large random matrices often converge to a fixed asymptotic distribution. This important property can be used to derive analytical rate expressions. Through LSA, Gomadam *et al.* [14] have derived the asymptotic capacity of a wireless communication system with multiple transmit and receive antennas. In [15], by using LSA the authors calculated the probability distribution of the mutual information of MIMO channels with large but limited antenna numbers. The paper [16] proposed a method based on the combination of some large random matrix results with convex optimization, and derived the cellular network system capacity with LSA. In a two-cell system [17], through LSA the SINR and bit-error rate expressions are obtained. Also in [18], the rate expressions of interference alignment (IA) were derived through the LSA for the multiple-input multiple-output interference channel.

Stochastic geometry [19]–[21] is a very powerful mathematical and statistical tool for the modeling, analysis, and design of wireless networks with random topologies. In this paper, we employ stochastic geometry analysis for heterogeneous cellular networks, where a single macro base station (MaBS) with multiple transmitting antennas coexists with several micro base stations (MiBSs) whose spatial distribution obey a Poisson point processes(PPP). In order to improve the performance of HCNs, we perform interference alignment via rank constrained rank minimization (RCRM) [22]–[24] to cancel both intra-tier interferences from the MaBS to the MaUEs and cross-tier interferences from the MaBS to the MiUEs. The large system analysis (LSA) is then used to compute the achievable rates of the users in HCNs through LSA. In particular, we derive the rate expressions of macro users (MaUEs) and micro users (MiUEs) through finding the asymptotic eigenvalue distribution of the channel gains with random matrix theory [25]. The obtained rate expressions of macro users (MaUEs) and micro users (MiUEs) are given as functions of the transmit power, noise power, MiBS density, and the transmission distance. Numerical results show the effectiveness of our derived rate expressions.

The main contributions of this paper are summarized as follows:

(1) We propose an HCN model, where a single MaBS with multiple transmitting antennas coexists with several closed-access MiBSs whose spatial distribution follows Poisson point processes (PPP). We also take into account the realistic path loss effect in our channel modeling that is established on the basis of stochastic geometry and can describe the topological randomness in the HCNs.

(2) We propose a RCRM-based interference alignment scheme in HCNs to design the precoding matrix of the transmitter and the beamforming matrix of the receiver to suppress the intra-tier interference from the MaBS to the MaUEs as well as the cross-tier interference from the MaBS to the MiUEs. The scheme can significantly improve the rate performance of MaUE and MiUE in HCNs.

(3) We conduct large system analysis (LSA) of the HCN and derive the rate expressions of the macro users (MaUEs) and micro users (MiUEs) in a closed-form.

The rest of the paper is organized as follows: Section II presents the system model. Section III introduces the interference alignment through rank constrained rank minimization. Section IV derives the rate expression of MaUE and that of MiUE in the HCNs through the LSA. Section V presents simulation results with discussions. Finally, we conclude our paper in Section VI.

Throughout this paper, the following notations are used: lowercase bold letters denote vectors while uppercase bold letters denote matrices. A^H represents the transpose of matrix A, $tr\,(A)$ represents the trace of matrix A, I_d represents the identity square matrix of size $d \times d$, and $\log\,(x)$ represents the base 2 logarithm. $N_c\,(\mu, C)$ denotes a circularly symmetric Gaussian distribution with mean vector μ and covariance matrix C.

II. SYSTEM MODEL

We consider a heterogeneous cellular network (HCN) as shown in Fig.1, where a single MaBS is underlaid with a random number Ω of close-access MiBSs. The MaBS has M_1 antennas and serves m_1 macro users (MaUEs) each equipped with N antennas in a circular region $\prod$ of radius r_1. The MiBSs are spatially distributed according to a homogeneous Poisson point process (PPP) Π_0 with intensity λ. Each MiBS, equipped with M_2 antennas, covers a circular cell of radius r_2 and serves one micro user (MiUE) which is uniformly distributed on the circumference of the cell. Let d be the number of data streams transmitted by all users.

A. MACRO TIER AND MICRO TIER MODEL

In the macro cell tier, assume that the available spectrum is split into B subchannels, each with bandwidth W hertz (Hz) and the MaBS uses all these subchannels to serve m_1 N-antenna MaUEs.

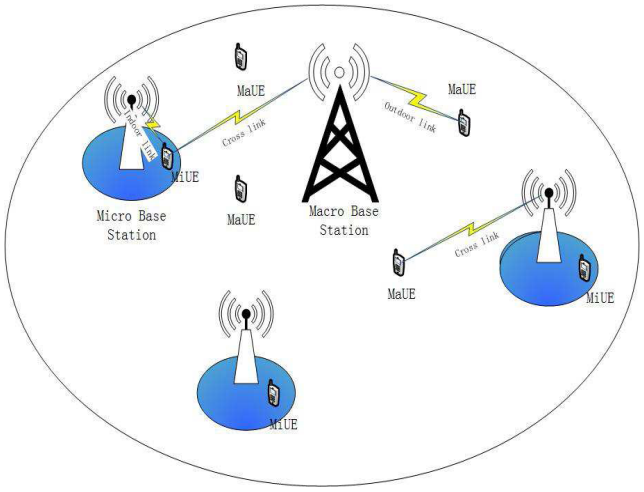

FIGURE 1. A heterogeneous cellular networks with a single MaBS which is under laid with a random number of closed-access MiBSs, with multiple antennas at both the MaUEs and MiUEs.

In the micro cell tier, assume that each MiBS employs time-division multiple-access (TDMA) as the multiple-access scheme to serve its N-antenna MiUE at each time slot.

B. CHANNEL MODEL

Suppose that the downlink channels at both tiers suffer from a path loss and Rayleigh fading. The path loss function at a distance r is described by $r^{-\alpha}$, with α being the path loss exponent. We denote α_1, α_2 and α_3 as the path loss exponents of the outdoor link, the indoor link and the cross link between indoor and outdoor, respectively. For the macrocell tier, we denote $G_i \in C^{N\times M_1}$ $(i = 1, \cdots, m_1)$ as the random channel matrices from MaBS to the i-th MaUE, and denote $G^j \in C^{N\times M_1}$ $(j = 1, \cdots, \Omega)$ as the random channel matrices from MaBS to the MiUE of the j-th MiBS. For the micro cell tier, we denote $K_{ij} \in C^{N\times M_2}$ $(i = 1, \cdots, m_1; j = 1, \cdots, \Omega)$ as the random channel matrices from the j-th MiBS to i-th MaUE, and denote $H_{jk} \in C^{N\times M_2}$ $(k = 1, \cdots, \Omega; j = 1, \cdots, \Omega)$ as the random channel matrices from the k-th MiBS to the MiUE of the j-th MiBS. The individual entries of all the links are i.i.d. Gaussian random variables obeying N_c (0, 1) distribution.

C. SIGNAL MODEL

Let x_i be the signal to be transmitted by the MaBS which is intended for the i-th MaUE, and s_j the signal to be transmitted by the j-th MiBS which is intended for its MiUE. Then, the signal received at the i-th MaUE can be written as

$$y_i = D_i^{-\alpha_1/2} G_i F_i x_i + \sum_{j=1}^{\Omega} \left(R_{ij}\right)^{-\alpha_3/2} K_{ij} V_j s_j + \sum_{k=1,k\neq i}^{m_1} D_i^{-\alpha_1/2} G_i F_k x_k + n_{1i} \quad (1)$$

where D_i is the distance from the MaBS to the i-th MaUE, R_{ij} is the distance from the j-th MiBS to the i-th MaUE, $F_i \in C^{M_1\times d}$ is the transmit precoding matrix from the MaBS to the i-th MaUE, $V_j \in C^{M_2\times d}$ is the transmit precoding matrix from the j-th MiBS to its MiUE, and n_{1i} is an N-dimensional complex additive white Gaussian noise (AWGN) vector with zero mean and covariance matrix $N_0 I_N$ with I_N being the identity matrix of dimension N.

Similarly, the signal received at the MiUE of the j-th MiBS can be written as

$$t_j = \left(R^{jj}\right)^{-\alpha_2/2} H_{jj} V_j s_j + \sum_{k=1,k\neq j}^{\Omega} \left(R^{jk}\right)^{-\alpha_3/2} H_{jk} V_k s_k + \left(D^j\right)^{-\alpha_1/2} G^j \sum_{k=1}^{m_1} F_k x_k + n_{2i} \quad (2)$$

where D^j is the distance from the MaBS to the MiUE of the j-th MiBS, R^{jk} is the distance from k-th MiBS to the MiUE of the j-th MiBS, and n_{2i}, similar to n_{1i} in (1), is an N-dimensional complex AWGN vector with zero mean and covariance matrix $N_0 I_N$.

D. INTERFERENCE ALIGNMENT FEASIBILITY CONDITIONS

Let the beamforming matrix of the receiver at the i-th MaUE and that at the MiUE of the j-th MiBS be given by $U_i \in C^{d\times N}$ $(i = 1, \cdots, m_1)$ and $W_j \in C^{d\times N}$ $(j = 1, \cdots, \Omega)$, respectively. Because of the random number of MiBSs and their random deployment, it is difficult to suppress all the interferences from the MiBSs. Using IA, we can suppress the intra-tier interference from the MaBS to the MaUEs and the cross-tier interference from the MaBS to the MiUEs. From equation (1) we can have the interference alignment conditions of MaUE as follows:

$$rank\,(U_i G_i F_i) = d, \quad i = 1, \cdots m_1 \quad (3)$$

$$U_i G_i F_k = 0, \quad i = 1, \cdots, m_1,\ k = 1, \cdots, m_1,\ k \neq i \quad (4)$$

Similarly, from equation (2) we obtain the following interference alignment conditions of MiUE:

$$rank\left(W_j H_{jj} V_j\right) = d, \quad j = 1, \cdots, \Omega \quad (5)$$

$$W_j G^j F_k = 0, \quad k = 1, \cdots m_1,\ j = 1, \cdots, \Omega \quad (6)$$

In this paper, we use IA to design the precoding matrix of the transmitter and the beamforming matrix of the receiver to align the interferences, and the details of the scheme will be presented in section III.

Based on algebraic geometry, it is well known that a generic system of multivariate polynomial equations is solvable if and only if the number of equations does not exceed the number of variables, so we explore the feasibility of interference alignment [26] through accurately accounting for the number of equations and the number of variables.

Define N_{v1} and N_{e1} as the number of variables and the number of equations of MaUE in the achievability conditions in (3) and (4), respectively. It can easily be verified that N_{e1} is given by:

$$N_{e1} = (m_1 \times m_1 - m_1)\, d^2 \tag{7}$$

and the total number of variables at MaUE is

$$N_{v1} = \sum_{i=1}^{m_1} d\,(M_1 - d + N - d) \tag{8}$$

Similarly, define N_{v2} and N_{e2} as the number of variables and that of equations of MiUE in the achievability conditions in (5) and (6), respectively. It can be shown that N_{e2} is given by:

$$N_{e2} = (\Omega \times m_1)\, d^2 \tag{9}$$

and the total number of variables at MiUE is

$$N_{v2} = \sum_{i=1}^{m_1} d\,(M_1 - d) + \sum_{i=1}^{\Omega} d\,(N - d) \tag{10}$$

By comparing the total number of equations and the total number of variables, we need:

$$N_{v1} \geq N_{e1} \tag{11}$$

and

$$N_{v2} \geq N_{e2} \tag{12}$$

then through calculation we have the feasibility conditions of interference alignment as follows:

$$M_1 + N \geq (m_1 + 1)\, d \tag{13}$$

and

$$m_1 M_1 + \Omega N \geq (\Omega \times m_1 + m_1 + \Omega)\, d \tag{14}$$

E. ACHIEVABLE RATES OF MAUES AND MIUES

For the ease of derivations, we assume $M_1 = M_2 = N$, we divide all the channel matrices by $\sqrt{d}$, namely,

$$\overline{G}_i = \frac{G_i}{\sqrt{d}}, \overline{G}_i \sim N_c\,(0, 1/d) \tag{15}$$

$$\overline{G}^j = \frac{G^j}{\sqrt{d}}, \overline{G}^j \sim N_c\,(0, 1/d) \tag{16}$$

$$\overline{K}_{ij} = \frac{K_{ij}}{\sqrt{d}}, \overline{K}_{ij} \sim N_c\,(0, 1/d) \tag{17}$$

$$\overline{H}_{jk} = \frac{H_{jk}}{\sqrt{d}}, \overline{H}_{jk} \sim N_c\,(0, 1/d) \tag{18}$$

and multiply the precoding matrix by $\sqrt{d}$, i.e.,

$$\overline{F}_i = \sqrt{d} F_i = F_{u,i} \left(\sqrt{d} P_i^{\frac{1}{2}}\right) \tag{19}$$

$$\overline{V}_j = \sqrt{d} V_j = V_{u,j} \left(\sqrt{d} \left(P^j\right)^{\frac{1}{2}}\right) \tag{20}$$

where $F_{u,i}$ and $V_{u,j}$ are unitary matrices, $P_i \in C^{M_1 \times d}$ and $P^j \in C^{M_2 \times d}$ are diagonal matrices containing the power assigned to the different streams on its main diagonal.

Then, we define the effective channel [18] of the above channel matrices as:

$$G_{i,eff} = U_i \overline{G}_i F_{u,i} \tag{21}$$

$$K_{ij,eff} = U_i \overline{K}_{ij} V_{u,j} \tag{22}$$

$$H_{jk,eff} = W_j \overline{H}_{jk} V_{u,k} \tag{23}$$

Through IA, we can get the rate of the i-th MaUE as follows [18]:

$$R_{MaUE,i} = \log\det\left(I_d + A_i\right) \tag{24}$$

where

$$A_i = \left(II_{MiBS\_MaUE,i} + N_0 I_d\right)^{-1} D_i^{-\alpha_1} G_{i,eff}^H G_{i,eff} \overline{P}_i,$$

with

$$II_{MiBS\_MaUE,i} = \sum_{j=1}^{\Omega} R_{ij}^{-\alpha_3} K_{ij,eff}^H K_{ij,eff} \overline{P}^j,$$

$$\overline{P}_i = d\left(P_i^{\frac{1}{2}}\right)^H \left(P_i^{\frac{1}{2}}\right) = diag\left(p_{i,1}, p_{i,2}, \cdots, p_{i,d}\right),$$

$$\overline{P}^j = d\left(\left(P^j\right)^{\frac{1}{2}}\right)^H \left(\left(P^j\right)^{\frac{1}{2}}\right) = diag\left(p_1^j, p_2^j, \cdots, p_d^j\right).$$

Note that $tr\left(\overline{P}_i\right) = Q_i$ and $tr\left(\overline{P}^j\right) = Q^j$, where Q_i and Q^j are the transmit power constraints.

Similarly, we can get the rate of the j-th MiUE through IA as follows:

$$R_{MiUE,j} = \log\det\left(I_d + B_j\right) \tag{25}$$

where

$$B_j = \left(II_{MiBS\_MiUE} + N_0 I_d\right)^{-1} \left(R^{jj}\right)^{-\alpha_2} \left(H_{jj,eff}\right)^H H_{jj,eff} P^j,$$

with

$$II_{MiBS\_MiUE} = \sum_{k=1, k\neq j}^{\Omega} \left(R^{jk}\right)^{-\alpha_3} \left(H_{jk,eff}\right)^H H_{jk,eff} \overline{P}^k.$$

III. INTERFERENCE ALIGNMENT THROUGH RANK CONSTRAINED RANK MINIMIZATION

In order to maximize the available DoF, A new method of implementing IA based on reformulation of the IA conditions via rank constrained rank minimization (RCRM) has been introduced recently in [22]. The idea of rank minimization is to maximize the interference alignment so that the interference spans a subspace of minimum dimension, and the rank constraints correspond to the useful signal subspaces satisfying full-rank constraints. An RCRM-based reweighed nuclear norm minimization algorithm has been presented to implement IA for MIMO system in [23]. Sridharan and Yu [24] have also proposed several variations of RCRM to design aligned beamformers in a cellular network. As shown in [23] and [24], in some cases the

RCRM outperforms previous approaches in designing transmit precoding and receive beamforming matrices for interference alignment. In this section, in order to improve the users rate performance of HCNs, we propose a RCRM-based interference alignment scheme to design the precoding matrix of the transmitter and the beamforming matrix of the receiver to suppress both the intra-tier interference and the cross-tier interference.

In HCNs, the macro-tier signal and interference (MaBS to MaUE) matrices at the i-th MaUE are defined as

$$S_{MaUE,i} = U_i G_i F_i, \quad i = 1, \cdots m_1 \tag{26}$$

$$II_{MaUE,i} = \begin{bmatrix} U_i G_1 F_1 \\ \vdots \\ U_i G_{k-1} F_{k-1} \\ U_i G_{k+1} F_{k+1} \\ \vdots \\ U_i G_{m_1} F_{m_1} \end{bmatrix}, \quad i = 1, \cdots, m_1; 1 < k \leq m_1 \tag{27}$$

Similarly, the micro-tier signal and interference (MaBS to MiUE) matrices at the j-th MiUE are defined as

$$S_{MiUE,j} = W_j H_{jj} V_j, \quad j = 1, \cdots, \Omega \tag{28}$$

$$II_{MiUE,j} = \begin{bmatrix} W_j G^j F_1 \\ \vdots \\ W_j G^j F_{k-1} \\ W_j G^j F_{k+1} \\ \vdots \\ W_j G^j F_{m_1} \end{bmatrix}, \quad j = 1, \cdots, \Omega; 1 < k \leq m_1 \tag{29}$$

From the interference alignment conditions (3) to (5), we can see that the interference alignment problem in HCNs is to solve $m_1 + \Omega$ optimization problems at the same time, which is however impossible. To tackle this difficulty, we turn to maximize the sum of interference free dimensions through RCRM. Then the optimization problems are formulated as:

$$\begin{aligned} &\min_{U_i, F_i} \sum_{i=1}^{m_1} rank(II_{MaUE,i}) \\ &s.t.\ rank(S_{MaUE,i}) = d, i = 1, \cdots, m_1 \end{aligned} \tag{30}$$

$$\begin{aligned} &\min_{W_i, V_i, F_i} \sum_{j=1}^{\Omega} rank\left(II_{MiUE,j}\right) \\ &s.t.\ rank(S_{MiUE,j}) = d, j = 1, \cdots, \Omega \end{aligned} \tag{31}$$

As the rank function in the above optimization problem is non-convex and NP-hard, the RCRM problem cannot be solved efficiently. Inspired by the compressed sensing and low-rank matrix completion theory [27], [28], the nuclear norm is chosen as a convex surrogate for the cost function and the rank constraints are replaced by Hermitian positive semi-definite matrix. Then the optimization problems are reformulated as:

$$\begin{aligned} &\min_{U_i, F_i} \sum_{i=1}^{m_1} \left\| II_{MaUE,i} \right\|_* \\ &s.t.\ S_{MaUE,i} \succeq 0_{d \times d}, \\ &\quad \theta_{\min}\left(S_{MaUE,i}\right) \geq \varepsilon, i = 1, \cdots, m_1. \end{aligned} \tag{32}$$

$$\begin{aligned} &\min_{W_j, V_j, F_i} \sum_{j=1}^{\Omega} \left\| II_{MiUE,j} \right\|_* \\ &s.t.\ S_{MiUE,j} \succeq 0_{d \times d}, \\ &\quad \theta_{\min}\left(S_{MiUE,j}\right) \geq \varepsilon, j = 1, \cdots, \Omega \end{aligned} \tag{33}$$

where $\|A\|_* = \sum_{t=1}^{rank(A)} \theta_t(A)$ is the nuclear norm of matrix A, which accounts for the sum of the singular values of A, and $\theta_t(A)$ is the t-th largest singular value of A. $S_i \succ 0_{d \times d}$ denotes that matrix S_i is Hermitian positive definite, and $\theta_{\min}(S_i)$ is the minimum eigenvalue of S_i, $\varepsilon > 0$.

To avoid the bilinear terms, we use the alternating minimization method in [7] to solve the above problems by optimizing the precoding and beamforming matrices alternately. From the aforementioned discussion, we can summarize the major steps of the IA via RCRM for designing the precoding matrices of the transmitter and the beamforming matrices of the receiver in Table 1.

TABLE 1. Interference Alignment algorithm via RCRM in HCNs.

1.Initialization: set arbitrary unitary matrix $\mathbf{F}_i$ and $\mathbf{V}_j$;
2.For the s-th iteration,
(i) with fixed $\mathbf{F}_i$, solve problem (32), giving $\mathbf{U}_i$;
(ii) with known $\mathbf{U}_i$, solve problem (32), giving $\mathbf{F}_i$;
(iii) by substituting $\mathbf{F}_i$ into optimal problem (33), and fixing $\mathbf{V}_j$, solve problem (33),giving $\mathbf{W}_j$;
(iv) with known $\mathbf{W}_j$ and $\mathbf{F}_i$, solve again problem (33) to obtain $\mathbf{V}_j$;
End for.
3. Output: $\mathbf{U}_i$, $\mathbf{F}_i$, $\mathbf{W}_j$, $\mathbf{V}_j$.

IV. ACHIEVABLE RATES THROUGH LARGE SYSTEM ANALYSIS

Here we carry out large system analysis to obtain the rate expressions. Let M_1, M_2 and N approach infinity, but with a constant ratio $M_i/N (i = 1, 2)$, namely,

$$M_1 \to \infty, \quad N \to \infty, with\ \beta_1 = \frac{M_1}{N} \tag{34}$$

$$M_2 \to \infty, \quad N \to \infty, with\ \beta_2 = \frac{M_2}{N} \tag{35}$$

As before, we assume $M_1 = M_2 = N$, so that $\beta_1 = \beta_2 = 1$, and also assume equal power is allocated to each

stream, namely,

$$p_{i,1} = p_{i,2} \ldots = p_{i,d} = \frac{Q_i}{d} = p_i \tag{36}$$

$$p_1^j = p_2^j = \cdots = p_d^j = \frac{Q^j}{d} = p^j \tag{37}$$

A. AVERAGE ACHIEVABLE RATE OF MAUE

Substituting equations (36) and (37) into (24), the rate of the i-th MaUE can be written as

$$R_{MaUE,i} = \sum_{l=1}^{d} \log\left(1 + \left(S_{MaUE} + II_{MiBS-MaUE}\right)/N_0\right) - \sum_{l=1}^{d} \log\left(1 + II_{MiBS-MaUE}/N_0\right) \tag{38}$$

where $S_{MaUE} = p_i D_i^{-\alpha_1} \theta_l \left(G_{i,eff}^H G_{i,eff}\right)$, $II_{MiBS-MaUE} = \sum_{j=1}^{\Omega} R_{ij}^{-\alpha_3} p^j \theta_l \left(K_{ij,eff}^H K_{ij,eff}\right)$.

As $d \to \infty$, under LSA the average achievable rate of MaUE is defined as [24]

$$R_{MaUE} = \lim_{d\to\infty} \frac{R_{MaUE,i}}{d} \tag{39}$$

So we have the following average achievable rate expression for MaUE,

$$R_{MaUE} = E\left(\log\left(1 + \left(S_{MaUE} + II_{MiBS-MaUE}\right)/N_0\right)\right) - E\left(\log\left(1 + II_{MiBS-MaUE}/N_0\right)\right) \tag{40}$$

For notational simplicity, we use G, K and H to denote $G_{i,eff}^H G_{i,eff}$, $K_{ij,eff}^H K_{ij,eff}$ and $H_{jk,eff}^H H_{jk,eff}$, respectively. Suppose that the MaBS serves a circular region $\prod$ of radius r_1, and the MiBSs are spatially distributed according to a homogeneous Poisson point process (PPP) with intensity λ. Using the conditional expectation formula, we can obtain the first term on the right side of equation (40) as:

$$R_{MaUE}\left(term\ I\right) = \sum_{m=1}^{\infty} E\left(\log\left(1 + \left(S_{MaUE} + II_{MiBS-MaUE}\right)/N_0\right)\right) P\left(m\right) \tag{41}$$

where $P(m)$ denote the the probability of finding m nodes in a circular region $\prod$.

Remark: Since the MaUE suffers the interference from MiBSs, so it must satisfied $m \geq 1$.

In a homogeneous 2-dimensional Poisson point process of intensity λ, the probability of finding m nodes in a circular region $\prod$ of radius r_1 is [29]:

$$P\left(m\ nodes\ in\ \prod\right) = e^{-\lambda\pi r_1^2} \frac{\left(\lambda\pi r_1^2\right)^m}{m!} \tag{42}$$

By substituting (42) into (41), letting $a = \frac{p_i D_i^{-\alpha_1}}{N_0}$ and $b = \frac{m r^{-\alpha_3} p^j}{N_0}$, and using the Shannon transform of random matrix theory [25], the equation (41) can be expressed as:

$$R_{MaUE}(term\ I) = \sum_{m=1}^{\infty} v_{G+\frac{b}{a}K}\left(a\right) e^{-\lambda\pi r_1^2} \frac{\left(\lambda\pi r_1^2\right)^m}{m!} \tag{43}$$

where $v_A\left(x\right)$ denotes the Shannon transform of matrix A. The definition of the Shannon transform is given in Appendix A.

In a manner similar to deriving (43), the second-term on the right side of (40) can be obtained as

$$R_{MaUE}(term\ II) = -\sum_{m=1}^{\infty} v_K\left(b\right) e^{-\lambda\pi r_1^2} \frac{\left(\lambda\pi r_1^2\right)^m}{m!} \tag{44}$$

Then, equation (40) can be expressed as:

$$R_{MaUE} = \sum_{m=1}^{\infty} v_{G+\frac{b}{a}K}\left(a\right) e^{-\lambda\pi r_1^2} \frac{\left(\lambda\pi r_1^2\right)^m}{m!} - \sum_{m=1}^{\infty} v_K\left(b\right) e^{-\lambda\pi r_1^2} \frac{\left(\lambda\pi r_1^2\right)^m}{m!} \tag{45}$$

The computation of the integrals on the right side of (45) leads to the following closed-form expression for the rate of MaUE (see Appendix B for detail)

$$\begin{aligned} R_{MaUE} &= 1.52 \log\left(\frac{p_i D_i^{-\alpha_1}}{N_0}\right) - \frac{\log e}{3} \frac{1}{\frac{p_i D_i^{-\alpha_1}}{N_0}} + \log\left(e\right) \\ &\quad - \sum_{m=1}^{\infty} 2\left(\log\left(0.5 + \sqrt{\frac{m r^{-\alpha_3} p^j}{N_0}}\right)\right) e^{-\lambda\pi r_1^2} \frac{\left(\lambda\pi r_1^2\right)^m}{m!} \\ &\quad + \frac{\log e}{6} \sum_{m=1}^{\infty} \frac{1}{\frac{m r^{-\alpha_3} p^j}{N_0}} e^{-\lambda\pi r_1^2} \frac{\left(\lambda\pi r_1^2\right)^m}{m!} \\ &\quad - \sum_{m=1}^{\infty} \left(\frac{\log\left(e\right)}{\sqrt{\frac{m r^{-\alpha_3} p^j}{N_0}}}\right) e^{-\lambda\pi r_1^2} \frac{\left(\lambda\pi r_1^2\right)^m}{m!} \end{aligned} \tag{46}$$

B. AVERAGE ACHIEVABLE RATE OF MIUE

Using the assumptions in (34)-(37) into (25), the j-th MiUE rate can be written as

$$R_{MiUE,j} = \sum_{l=1}^{d} \log\left(1 + \left(S_{MiUE} + II_{MiBS-MiUE}\right)/N_0\right) - \sum_{l=1}^{d} \log\left(1 + II_{MiBS-MiUE}/N_0\right) \tag{47}$$

where $S_{MiUE} = p^j \left(R^{jj}\right)^{-\alpha_2} \theta_l\left(H\right)$, $II_{MiBS-MiUE} = \sum_{k=1,k\neq j}^{\Omega} p^k \left(R^{jk}\right)^{-\alpha_3} \theta_l\left(H\right)$.

Using LSA, the average achievable rate of MiUE can be rewritten as

$$R_{MiUE} = E\left(\log\left(1 + \left(S_{MiUE} + II_{MiBS-MiUE}\right)/N_0\right)\right) - E\left(\log\left(1 + II_{MiBS-MiUE}/N_0\right)\right) \tag{48}$$

By letting $g = \frac{p^j (R^{ij})^{-\alpha_2}}{N_0}$ and $h = \frac{(m-1)p^k (R^{jk})^{-\alpha_3}}{N_0}$, and using the conditional expectation formula along with the Shannon transform of random matrix theory [22], equation (48) can be transformed to

$$R_{MiUE} = \sum_{m=2}^{\infty} v_H\,(g+h)\, e^{-\lambda\pi r_1^2} \frac{\left(\lambda\pi r_1^2\right)^m}{m!} - \sum_{m=2}^{\infty} v_H\,(h)\, e^{-\lambda\pi r_1^2} \frac{\left(\lambda\pi r_1^2\right)^m}{m!} \quad (49)$$

Remark: Since the MiUE suffers the interference from other MiBSs, so it must satisfy $m \geq 2$.

Computing the integrals in (49) results in a closed-form rate expression of MiUE as given by

$$\begin{aligned} R_{MiUE} &= \sum_{m=2}^{\infty} \left(\log\left(\left(R^{jj}\right)^{-\alpha_2} + (m-1)\left(R^{jk}\right)^{-\alpha_3} \right) \right) e^{-\lambda\pi r_1^2} \frac{\left(\lambda\pi r_1^2\right)^m}{m!} \\ &\quad - \sum_{m=2}^{\infty} \left(\log\left((m-1)\left(R^{jk}\right)^{-\alpha_3} \right) \right) e^{-\lambda\pi r_1^2} \frac{\left(\lambda\pi r_1^2\right)^m}{m!} \\ &\quad - \sum_{m=2}^{\infty} \frac{\log(e)\, e^{-\lambda\pi r_1^2} \frac{\left(\lambda\pi r_1^2\right)^m}{m!}}{2\left(\frac{p^j (R^{ij})^{-\alpha_2}}{N_0} + \frac{(m-1)p^k (R^{jk})^{-\alpha_3}}{N_0} \right)} \\ &\quad + \sum_{m=2}^{\infty} \frac{\log(e)\, e^{-\lambda\pi r_1^2} \frac{\left(\lambda\pi r_1^2\right)^m}{m!}}{\sqrt{\frac{p^j (R^{ij})^{-\alpha_2}}{N_0} + \frac{(m-1)p^k (R^{jk})^{-\alpha_3}}{N_0}}} \\ &\quad + \sum_{m=2}^{\infty} \log(e)\, \frac{e^{-\lambda\pi r_1^2} \frac{\left(\lambda\pi r_1^2\right)^m}{m!}}{2\frac{(m-1)p^k (R^{jk})^{-\alpha_3}}{N_0}} \\ &\quad - \sum_{m=2}^{\infty} \frac{\log(e)\, e^{-\lambda\pi r_1^2} \frac{\left(\lambda\pi r_1^2\right)^m}{m!}}{\sqrt{\frac{(m-1)p^k (R^{jk})^{-\alpha_3}}{N_0}}} \end{aligned} \quad (50)$$

The detailed derivation is given in Appendix C.

V. SIMULATION RESULTS AND DISCUSSION

In this section, we carry out simulation studies to illustrate the effectiveness of the derived average achievable rates of MaUE and MiUE in the HCNs through the large system analysis. In our simulation, we suppose that Macro BS is placed at the center of a circular region with radius r_1. We assume $d = N/2$, and the MaUE number, the MiUE number, the MaUE antenna number, and the MiUE antenna number set satisfied (13) and (14). Unless otherwise stated, other system parameters are shown in Table 2. We use red lines to depict the average achievable rate through LSA and blue lines to depict the average achievable rate with fixed antenna numbers given in (24) and (25). Our simulation results are averaged over 1000 i.i.d. channel realizations, where the individual entries of all links are drawn from N_c (0, 1) distribution.

TABLE 2. system simulation parameters.

Parameter	Symbol	Value
Macro BS coverage radius	r_1	1Km
MaBS to the i-th MaUE distance	D_i	500m
From the j-th MiBS to the MiUE of the j-th MiBS distance	R^{jj}	30 m
Outdoor path loss exponent	α_1	3.8
Indoor path loss exponent	α_2	3.8
Indoor-to-outdoor path loss exponent	α_3	5.0
MaBS transmission power	Q_i	50 dBm
MiBS transmission power	Q^j	20 dBm
Noise power	N_0	10^{-7}
The number of MaUE	m_1	10

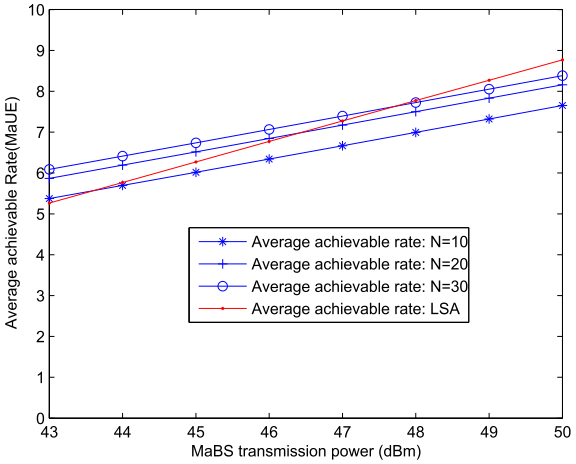

FIGURE 2. Average achievable rate at MaUE as a function of the MaBS transmission power.

A. AVERAGE ACHIEVABLE RATE OF MAUE

First, Fig. 2 shows the average achievable rate at MaUE as a function of the MaBS transmission power. Clearly, the average achievable rate resulting from LSA provides good approximations of the average achievable rates. Also, it increases when the MaBS transmission power is increased.

Fig.3 plots the average achievable rate of MaUE with respect to the MiBS density λ. It is shown that the average achievable rates through LSA provide good approximations of the average achievable rates. The average achievable rate of MaUE decreases as the MiBS density increases. This is mainly because the increase of the density of MiBS will cause more cross-tier interference, and thus the average achievable rate of MaUE will decrease.

Fig. 4 shows the average achievable rate at MaUE as a function of MaBS to the MaUE distance. We have observed a significant effect of the MaBS-to-MaUE distance on the average achievable rate of MaUE. This is due to the fact that the average achievable rate becomes much larger when the MaUEs is closer to the MaBS.

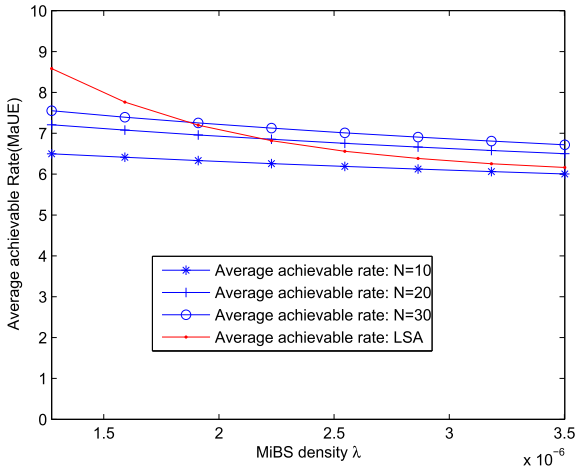

FIGURE 3. Average achievable rate at MaUE as a function of density λ.

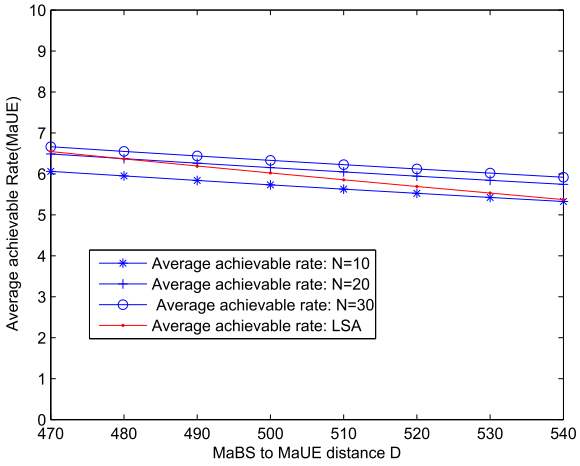

FIGURE 4. Average achievable rate at MaUE as a function of MaBS to the MaUE distanc.

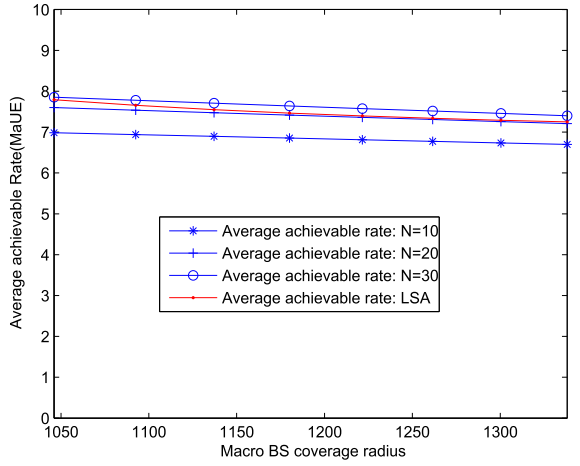

FIGURE 5. Average achievable rate at MaUE as a function of Macro BS coverage radius.

Fig.5 gives the average achievable rate at MaUE as a function of the Macro BS coverage radius, which shows a large effect of the Macro BS coverage radius on the performance.

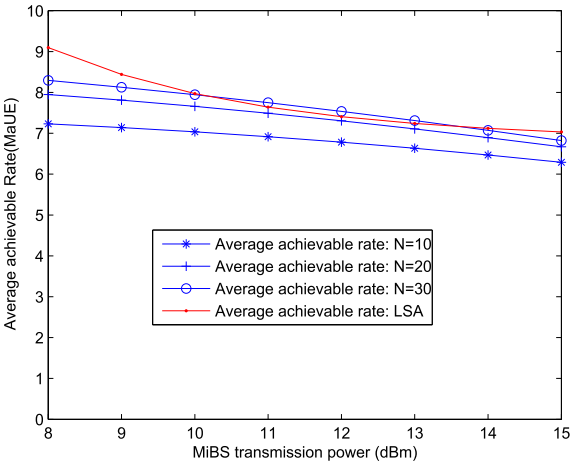

FIGURE 6. Average achievable rate at MaUE as a function of MiBS transmission power.

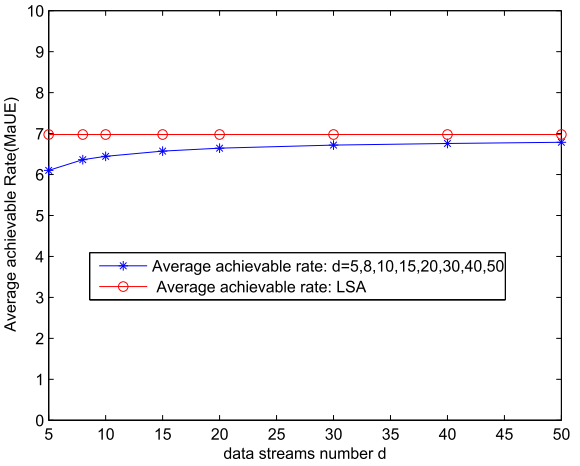

FIGURE 7. Average achievable rate at MaUE as a function of data streams numbers.

This is mainly because the number of MiBSs will in general increase as the Macro BS coverage radius increases, which in turn causes more cross-tier interference.

Fig. 6 depicts the average achievable rate at MaUE as a function of the MiBS transmission power. It is observed that as the MiBS transmission power increases the average achievable rate is decreased as expected.

Fig. 2 to Fig. 6 show the average achievable rate at MaUE compared with the antenna number limited cases. Clearly, the average achievable rate at MaUE provides a good asymptotic approximation to the numerical results under the finite number of antennas.

Fig.7 correspond to the performance of average achievable rate of MaUE versus the number of streams. We can see that the average achievable rate of MaUE converges to a fixed value with increasing the number of streams. With an increased number of streams, the average achievable rate through LSA always provides good estimates of the average achievable rates at any number of data streams.

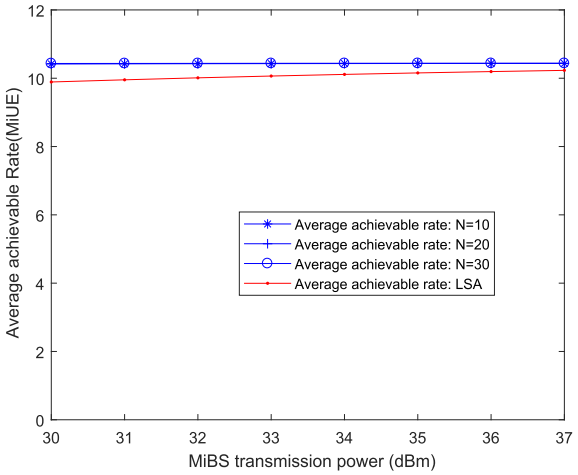

FIGURE 8. Average achievable rate at MiUE as a function of MiBS transmission power.

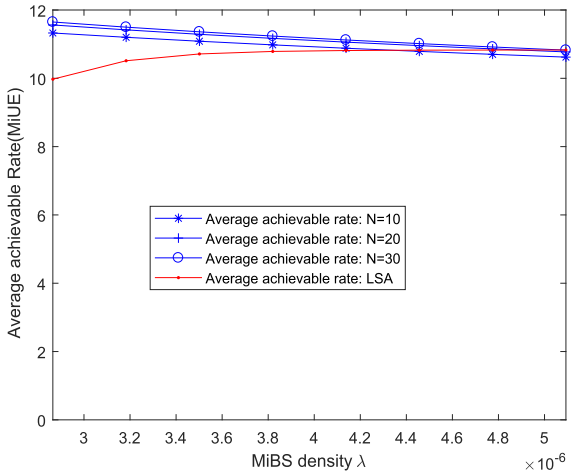

FIGURE 9. Average achievable rate at MiUE as a function of density λ.

B. AVERAGE ACHIEVABLE RATE OF MIUE

Here, we study the average achievable rate through LAS and the average rate versus different number of MiUEs's antennas. Moreover, the simulation results are provided to illustrate the effectiveness of the derived average achievable rate of MiUE.

Fig.8 illustrates the average achievable rate of MiUE plotted against MiBS transmission power. the average achievable rate at the MiUE has little change with increasing the the MiBS transmission power, this is mainly because the MiBS transmission power increase, also cause the interference signal power increase at the same time.

Fig.9 shows the average achievable rate of MiUE with respect to the MiBS density λ. As expected, the average achievable rate decrease as the MiBS density increased. This is mainly because the increase of the density of MiBSs will cause more intra-tier interference, that will reduce the average achievable rate.

Fig.10 shows the average achievable rate of MiUE as a function of MiBS to MiUE distance. As observed, the average achievable rate gets larger when MiUE is closer to the MiBS.

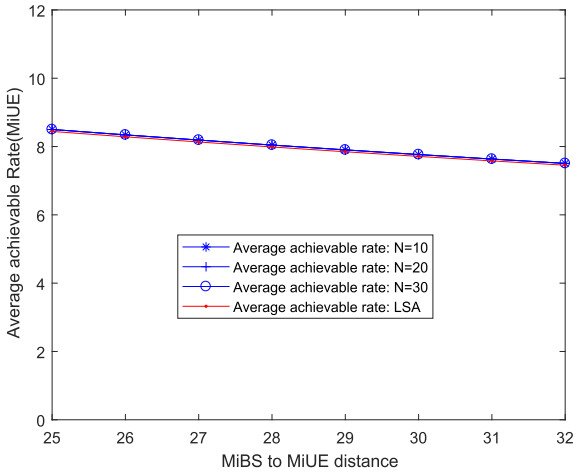

FIGURE 10. Average achievable rate at MiUE as a function of MiBS to MiUE distance.

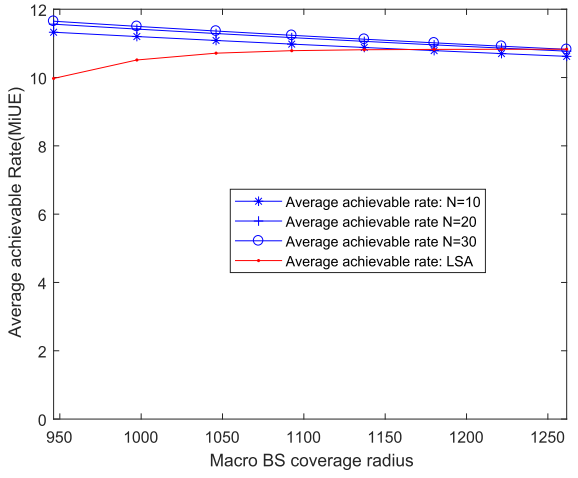

FIGURE 11. Average achievable rate at MiUE as a function of Macro BS coverage radius.

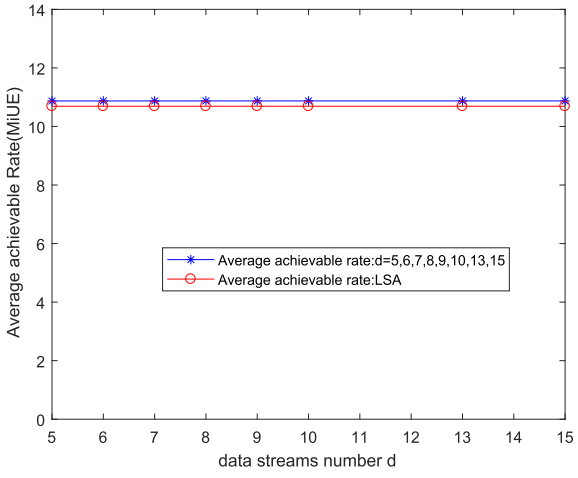

FIGURE 12. Average achievable rate at MiUE as a function of data streams numbers.

Fig.11 shows the average achievable rate of MiUE as a function of Macro BS coverage radius. Since the number of MiBSs will generally increase when the Macro

BS radius increases, which will cause more intra-tier interference, the average achievable rate of MiUE is thus reduced.

Fig.8 to Fig.11 show that the average achievable rate at MiUE resulting from LSA provides good asymptotic approximation to the numerical results under the finite number of antennas.

Fig.12 shows the average achievable rate of MiUE with respect to the data stream number. This figure indicates that the average achievable rate at the MiUE always converges to a fixed value when increasing the number of streams.

VI. CONCLUSION

In this paper, we have analysed the average achievable rates of an HCN composed of a single MaBS with multiple random access MiBSs and performed interference alignment by designing the transmit precoding and receive beamforming matrices via rank constrained rank minimization. Closed-form average achievable rate expressions have then been derived through large system analysis. The key to obtaining a closed-form rate expression is finding the asymptotic eigenvalue distribution of the resulting channel gains using the random matrix theory. The derived average achievable rate expressions for the macro users (MaUEs) and micro users (MiUEs) are found to be functions of the transmit power, noise power, the MiBS density and other system parameters. Extensive simulation studies have been conducted with all the results confirming the validity of the rate expressions derived through the large system analysis with interference alignment.

Appendix A
REQUIRED RANDOM MATRIX THEORY RESULTS

Here, we briefly introduce some of the random matrix theory results which are useful for the LSA in our paper.

A. The Marcenko-Pastur Distribution

Let A be a $s \times t$ complex random matrix with i.i.d. zero-mean elements of variance $1/s$. Let $\alpha = t/s$, as $s \to \infty, t \to \infty$ at a fixed ratio α, the distribution of the eigenvalues of AA^H converges almost surely to a fixed distribution with density [25]:

$$f(\lambda) = \left(1 - \frac{1}{\alpha}\right)^+ \delta(\lambda) + \frac{\sqrt{(\lambda - aa)^+ (\lambda - bb)^+}}{2\pi\alpha\lambda} \quad (51)$$

where $aa = \left(1 - \sqrt{\alpha}\right)^2$, $bb = \left(1 + \sqrt{\alpha}\right)^2$, and $y^+ = \max(0, y)$.

B. Shannon Transform

The Shannon transform of the eigenvalue distribution of a non-negative definite random matrix X is defined as [25]

$$v_X(\gamma) = E\left[\log(1 + \gamma X)\right] \quad (52)$$

where γ is a nonnegative real number.

If X follows an Marcenko-Pastur distribution, its Shannon transform can be found in a closed-form as

$$v_X(\gamma) = \log\left(1 + \gamma - \frac{1}{4}F(\gamma, \alpha)\right) + \frac{1}{\alpha}\log\left(1 + \gamma\alpha - \frac{1}{4}F(\gamma, \alpha)\right) - \frac{\log(e)}{4\gamma\alpha}F(\gamma, \alpha) \quad (53)$$

where $F(\gamma, \alpha) = \left(\sqrt{\gamma\left(1+\sqrt{\alpha}\right)^2+1} - \sqrt{\gamma\left(1-\sqrt{\alpha}\right)^2+1}\right)$.

C. η-transform

The η-transform of the eigenvalue distribution of a non-negative definite random matrix X is defined as [25]

$$\eta_X(\gamma) = E\left[\frac{1}{1 + \gamma X}\right] \quad (54)$$

where γ is a nonnegative real number.

D. R-transform

If a complex random matrix A of size $s \times t$ follows a Marcenko-Pastur distribution, its R-transform can be found in a closed-form as [25]:

$$R_A(x) = \frac{1}{1 - \alpha x} \quad (55)$$

where $\alpha = t/s$.

E. Relationship between the aforementioned transforms

(1)The relationship between Shannon transform and η-transform is given by [25]:

$$\frac{\gamma}{\log e}\frac{d}{d\gamma}v_X(\gamma) = 1 - \eta_X(\gamma) \quad (56)$$

(2)The relationship between R-transform and η-transform is stated as [25]:

$$\eta_X(\gamma) = \frac{1}{1 + \gamma R_X(-\gamma\eta_X(\gamma))} \quad (57)$$

Appendix B
DERIVATION OF MAUE RATE (46)

The key to computing equation (45) is to obtain the Shannon transforms of matrices $G + \frac{b}{a}K$ and K. Recall that U_i and W_j are unitary matrices, and the effective channel matrices G and K have the same distribution with $\bar{G_i}$ and $\bar{K_{ij}}$. In random matrix theory [25], as $d \to \infty$, the eigenvalue distribution of G and K converges almost surely to a Marcenko-Pastur distribution with $\alpha = 1$. Hence the R-transform of the random matrices G and K can be written as

$$R_G(z) = R_K(z) = \frac{1}{1 - z} \quad (58)$$

Further, we can obtain the R-transform of $G + \frac{b}{a}K$ as given below:

$$R_{G+\frac{b}{a}K}(z) = R_G(z) + \frac{b}{a}R_K(\frac{b}{a}z) = \frac{1}{1 - z} + \frac{\frac{b}{a}}{1 - \frac{b}{a}z} \quad (59)$$

The relationship between the R-transform and the η-transform is introduced in appendix A as (57). Letting $\delta = \frac{b}{a}, x = \eta_{G+\frac{b}{a}K}(\gamma)$, we can obtain the η-transform of $G+\frac{b}{a}K$ through solving the following equation

$$x^3 + \frac{\delta\gamma+\delta+1}{\delta\gamma}x^2 + \frac{x}{\delta\gamma^2} - \frac{1}{\delta\gamma^2} = 0 \tag{60}$$

with the help of Matlab calculation, we can have the value of x as

$$x = \sqrt[3]{\sqrt{tt^2+bb^3}+tt} - \frac{bb}{\sqrt[3]{\sqrt{tt^2+bb^3}+tt}} - \frac{t}{3\delta\gamma^2} \tag{61}$$

where $t = \gamma+\gamma\delta+\gamma^2\delta$, $bb = \frac{1}{3\delta\gamma^2} + \frac{t^2}{9\delta^2\gamma^4}$ and $tt = \frac{1}{2\delta\gamma^2} + \frac{t}{6\delta^2\gamma^4} - \frac{t^3}{27\delta^3\gamma^6}$.

let $\mu=\frac{1}{\delta\gamma^2}$, we can have

$$\begin{aligned} tt^2+bb^3 &= \left(\frac{2}{3}\mu - \frac{1}{27}\right)^2 + \left(\frac{1}{3}\mu+\frac{1}{9}\right)^3 \\ &= \frac{1}{27}(\mu+13)\left((\mu-0.0385)^2+0.0042\right) \\ &\approx \frac{13}{27}\left((\mu-0.0385)^2+0.0042\right) \end{aligned} \tag{62}$$

Assuming that $\mu \ll 0.0385$, for simplicity we can have the η-transform of $G+\frac{b}{a}K$ as given below:

$$\begin{aligned} &\eta_{G+\frac{b}{a}K} \\ &= \sqrt[3]{\frac{2}{3}\frac{1}{\delta\gamma^2}+0.0153} - \frac{\frac{1}{3\delta\gamma^2}+\frac{1}{9}}{\sqrt[3]{\frac{2}{3}\frac{1}{\delta\gamma^2}+0.0153}} - \frac{\gamma+\gamma\delta+\gamma^2\delta}{3\delta\gamma^2} \end{aligned} \tag{63}$$

By using the relationship between the Shannon transform and the η-transform in appendix A known as(56), we have

$$\begin{aligned} \frac{d}{d\gamma}v_X(\gamma) = \log(e)\Bigg(&\frac{1}{\gamma} - \frac{\sqrt[3]{\frac{2}{3}\frac{1}{\delta\gamma^2}+0.0153}}{\gamma} \\ &+ \frac{\frac{1}{3\delta\gamma^2}+\frac{1}{9}}{\gamma\sqrt[3]{\frac{2}{3}\frac{1}{\delta\gamma^2}+0.0153}} + \frac{1+\delta+\gamma\delta}{3\delta\gamma^2}\Bigg) \end{aligned} \tag{64}$$

According to previous assumption $\mu \ll 0.0385$, we have $\frac{1}{\delta\gamma^2} \ll 0.023$, direct computation of the above equation leads to the Shannon-transform of $G+\frac{b}{a}K$ as given by

$$v_{G+\frac{b}{a}K}(\gamma) = 1.52\log(\gamma) - \frac{1+\delta}{3\delta}\frac{\log e}{\gamma} \tag{65}$$

Substituting the value of a and b into the above equation, we obtain

$$\begin{aligned} v_{G+\frac{b}{a}K}(a) = 1.52\log\left(\frac{p_i D_i^{-\alpha_1}}{N_0}\right) \\ - \frac{\log e}{3}\left(\frac{1}{\frac{p_i D_i^{-\alpha_1}}{N_0}} + \frac{1}{\frac{mr^{-\alpha_3}p_1^j}{N_0}}\right) \end{aligned} \tag{66}$$

On the other hand, the random matrix K follows a Marcenko-Pastur distribution, so its Shannon transform [25] can be found in closed-form as

$$\begin{aligned} v_K(\gamma) = 2\log\left(\frac{1}{2}+\frac{\sqrt{4\gamma+1}}{2}\right) \\ - \log(e)\left(\frac{1}{2\gamma}+1\right) + \frac{\log(e)}{2\gamma}\sqrt{4\gamma+1} \end{aligned} \tag{67}$$

For simplicity, assuming $\gamma \gg 1$, we can have

$$v_K(\gamma) \approx 2\log\left(\frac{1}{2}+\sqrt{\gamma}\right) - \log(e)\left(\frac{1}{2\gamma}+1\right) + \frac{\log(e)}{\sqrt{\gamma}} \tag{68}$$

Substituting b into (68) gives

$$\begin{aligned} v_K(b) = 2\log\left(\frac{1}{2}+\sqrt{\frac{mr^{-\alpha_3}p_1^j}{N_0}}\right) \\ - \log(e)\left(\frac{1}{2\frac{mr^{-\alpha_3}p_1^j}{N_0}}+1\right) + \frac{\log(e)}{\sqrt{\frac{mr^{-\alpha_3}p_1^j}{N_0}}} \end{aligned} \tag{69}$$

Finally, substituting (66) and (69) into equation (45), we can have the MaUE average achievable rate expression in (46).

Appendix C
DERIVATION OF MIUE RATE (50)

Similar to the derivation of (46), our idea is to use the Shannon transform of matrix H. Recall that U_i and W_j are unitary matrices. So the effective channel matrices $H_{jk,eff}$ have the same distribution as H. From random matrix theory [25], the random matrix H follows a Marcenko-Pastur distribution, and its Shannon-transform can be found in a closed-form as:

$$v_H(\gamma) \approx 2\log\left(\frac{1}{2}+\sqrt{\gamma}\right) - \log(e)\left(\frac{1}{2\gamma}+1\right) + \frac{\log(e)}{\sqrt{\gamma}} \tag{70}$$

Substituting (70) into equation (49), we can have

$$\begin{aligned} &R_{MiUE} \\ &= \sum_{m=2}^{\infty}\left(2\log\left(0.5+\sqrt{g+h}\right)\right)e^{-\lambda\pi r_1^2}\frac{(\lambda\pi r_1^2)^m}{m!} \\ &+ \sum_{m=2}^{\infty}\left(-\log(e)\left(\frac{1}{2g+2h}+1\right)\right)e^{-\lambda\pi r_1^2}\frac{(\lambda\pi r_1^2)^m}{m!} \\ &+ \sum_{m=2}^{\infty}\left(\frac{\log(e)}{\sqrt{g+h}}\right)e^{-\lambda\pi r_1^2}\frac{(\lambda\pi r_1^2)^m}{m!} \\ &- \sum_{m=2}^{\infty}\left(2\log\left(0.5+\sqrt{h}\right)\right)e^{-\lambda\pi r_1^2}\frac{(\lambda\pi r_1^2)^m}{m!} \\ &- \sum_{m=2}^{\infty}\left(-\log(e)\left(\frac{1}{2h}+1\right)\right)e^{-\lambda\pi r_1^2}\frac{(\lambda\pi r_1^2)^m}{m!} \\ &- \sum_{m=2}^{\infty}\left(\frac{\log(e)}{\sqrt{h}}\right)e^{-\lambda\pi r_1^2}\frac{(\lambda\pi r_1^2)^m}{m!} \end{aligned} \tag{71}$$

Finally, substituting g and h into above equation yields the MiUE rate expression in (50).

REFERENCES

[1] J. Wen, M. Sheng, X. Wang, J. Li, and H. Sun, "On the capacity of downlink multi-hop heterogeneous cellular networks," *IEEE Trans. Wireless Commun.*, vol. 13, no. 8, pp. 4092–4103, Aug. 2014.

[2] S. Mukherjee, "Distribution of downlink SINR in heterogeneous cellular networks," *IEEE J. Sel. Areas Commun.*, vol. 30, no. 3, pp. 575–585, Mar. 2012.

[3] V. R. Cadambe and S. A. Jafar, "Interference alignment and degrees of freedom of the K-user interference channel," *IEEE Trans. Inf. Theory*, vol. 54, no. 8, pp. 3425–3441, Aug. 2008.

[4] K. Gomadam, V. R. Cadambe, and S. A. Jafar, "A distributed numerical approach to interference alignment and applications to wireless interference networks," *IEEE Trans. Inf. Theory*, vol. 57, no. 6, pp. 3309–3322, Jun. 2011.

[5] S. A. Jafar and M. J. Fakhereddin, "Degrees of freedom for the MIMO interference channel," *IEEE Trans. Inf. Theory*, vol. 53, no. 7, pp. 2637–2642, Jul. 2007.

[6] S. W. Peters and R. W. Heath, Jr., "Cooperative algorithms for MIMO interference channels," *IEEE Trans. Veh. Technol.*, vol. 60, no. 1, pp. 206–218, Jan. 2011.

[7] S. W. Peters and R. W. Heath, Jr., "Interference alignment via alternating minimization," in *Proc. IEEE Int. Conf. Acoust., Speech, Signal Process. (ICASSP)*, Taipei, Taiwan, Apr. 2009, pp. 2445–2448.

[8] N. Zhao, F. R. Yu, M. Jin, Q. Yan, and V. C. M. Leung, "Interference alignment and its applications: A survey, research issues, and challenges," *IEEE Commun. Surveys Tuts.*, vol. 18, no. 3, pp. 1779–1803, 3rd Quart., 2016.

[9] N. Zhao, X. Liu, F. R. Yu, M. Li, and V. C. M. Leung, "Communications, caching, and computing oriented small cell networks with interference alignment," *IEEE Commun. Mag.*, vol. 54, no. 9, pp. 29–35, Sep. 2016.

[10] N. Zhao, F. R. Yu, and V. C. M. Leung, "Opportunistic communications in interference alignment networks with wireless power transfer," *IEEE Wireless Commun.*, vol. 22, no. 1, pp. 88–95, Feb. 2015.

[11] D. Aziz, M. Mazhar, and A. Weber, "Interference management through interference alignment based transmit precoding in multi user heterogeneous cellular networks," in *Proc. Eur. Wireless, 20th Eur. Wireless Conf.*, 2014, pp. 1–6.

[12] S. Imam and A. El-Mahdy, "Selective interference alignment in 5G networks," in *Proc. Signal Process., Algorithms, Archit., Arrangements, Appl. (SPA)*, 2016, pp. 147–151.

[13] D. Aziz, M. Mazhar, and A. Weber, "Multi user inter cell interference alignment in heterogeneous cellular networks," in *Proc. IEEE 79th Veh. Technol. Conf. (VTC Spring)*, May 2014, pp. 1–5.

[14] A. Lozano and A. M. Tulino, "Capacity of multiple-transmit multiple-receive antenna architectures," *IEEE Trans. Inf. Theory*, vol. 48, no. 12, pp. 3117–3128, Dec. 2002.

[15] P. Kazakopoulos, P. Mertikopoulos, A. L. Moustakas, and G. Caire, "Distribution of MIMO mutual information: A large deviations approach," in *Proc. IEEE Inf. Theory Workshop Netw. Inf. Theory (ITW)*, Jun. 2009, pp. 306–310.

[16] H. Huh, A. Tulinoy, and G. Caire, "Network MIMO large-system analysis and the impact of CSIT estimation," in *Proc. 44th Annu. Conf. Inf. Sci. Syst. (CISS)*, 2010, pp. 1–6.

[17] R. Zakhour and S. V. Hanly, "Base station cooperation on the downlink: Large system analysis," *IEEE Trans. Inf. Theory*, vol. 58, no. 4, pp. 2079–2106, Apr. 2012.

[18] S. Bazzi, G. Dietl, and W. Utschick, "Large system analysis of interference alignment achievable rates for the MIMO interference channel," *IEEE Trans. Signal Process.*, vol. 63, no. 6, pp. 1490–1499, Mar. 2015.

[19] H. Elsawy, E. Hossain, and M. Haenggi, "Stochastic geometry for modeling, analysis, and design of multi-tier and cognitive cellular wireless networks: A survey," *IEEE Commun. Surveys Tuts.*, vol. 15, no. 3, pp. 996–1019, Jun. 2013.

[20] M. Haenggi, J. G. Andrews, F. Baccelli, O. Dousse, and M. Franceschetti, "Stochastic geometry and random graphs for the analysis and design of wireless networks," *IEEE J. Sel. Areas Commun.*, vol. 27, no. 7, pp. 1029–1046, Sep. 2009.

[21] T. M. Nguyen, Y. Jeong, T. Q. S. Quek, W. P. Tay, and H. Shin, "Interference alignment in a poisson field of MIMO femtocells," *IEEE Trans. Wireless Commun.*, vol. 12, no. 6, pp. 2633–2645, Jun. 2013.

[22] D. S. Papailiopoulos and A. G. Dimakis, "Interference alignment as a rank constrained rank minimization," *IEEE Trans. Signal Process.*, vol. 60, no. 8, pp. 4278–4288, Aug. 2012.

[23] H. Du, T. Ratnarajah, M. Sellathurai, and C. B. Papadias, "Reweighted nuclear norm approach for interference alignment," *IEEE Trans. Commun.*, vol. 61, no. 9, pp. 3754–3765, Sep. 2013.

[24] G. Sridharan and W. Yu, "Linear beamformer design for interference alignment via rank minimization," *IEEE Trans. Signal Process.*, vol. 63, no. 22, pp. 5910–5923, Nov. 2015.

[25] A. M. Tulino and S. Verdú, *Random Matrix Theory and Wireless Communications*. Boston, MA, USA: Now Publishers, 2004, pp. 168–189.

[26] C. M. Yetis, T. Gou, S. A. Jafar, and A. H. Kayran, "On feasibility of interference alignment in MIMO interference networks," *IEEE Trans. Signal Process.*, vol. 58, no. 9, pp. 4771–4782, Sep. 2010.

[27] B. Recht, M. Fazel, and P. A. Parrilo, "Guaranteed minimum-rank solutions of linear matrix equations via nuclear norm minimization," *SIAM Rev.*, vol. 52, pp. 471–501, Aug. 2010.

[28] E. J. Candès and T. Tao, "The power of convex relaxation: Near-optimal matrix completion," *IEEE Trans. Inf. Theory*, vol. 56, no. 5, pp. 2053–2080, May 2010.

[29] M. Haenggi, "On distances in uniformly random networks," *IEEE Trans. Inf. Theory*, vol. 51, no. 10, pp. 3584–3586, Oct. 2005.

XUE JIANG received the M. S. degree in 2007. She is currently pursuing the Ph.D. degree with the Nanjing University of Posts and Telecommunications, China. Her research interests include signal processing in wireless communications and interference alignment.

BAOYU ZHENG (SM'12) received the B.S. and M.S. degrees from the Department of Circuit and Signal System, Nanjing University of Posts and Telecommunications (NUPT), in 1969 and 1981, respectively. Since 1981, he has been engaged in teaching and researching in signal and information processing. He is currently a Full Professor and Doctoral Advisor with NUPT. His research interests span the broad area of the intelligent signal processing, wireless network and signal processing for modern communication, and the quantum signal processing.

WEI-PING ZHU (SM'97) received the B.E. and M.E. degrees from the Nanjing University of Posts and Telecommunications, Nanjing, China, and the Ph.D. degree from Southeast University, Nanjing, China, in 1982, 1985, and 1991, respectively, all in electrical engineering. He was a Post-Doctoral Fellow from 1991 to 1992 and from 1996 to 1998 as a Research Associate with the Department of Electrical and Computer Engineering, Concordia University, Montreal, QC, Canada. From 1993 to 1996, he was an Associate Professor with the Department of Information Engineering, Nanjing University of Posts and Telecommunications. From 1998 to 2001, he was with hi-tech companies in Ottawa, Canada, including Nortel Networks and SR Telecom Inc. Since 2001, he has been with Electrical and Computer Engineering Department, Concordia University as a full-time faculty member, where he is currently a Full Professor. Since 2008, he has been an Adjunct Professor with the Nanjing University of Posts and Telecommunications. His research interests include digital signal processing fundamentals, speech and statistical signal processing, and signal processing for wireless communication with a particular focus on MIMO systems and cooperative communication.

LEI WANG (M'15) received the M.Sc. degree and the Ph.D. degree in telecommunications and information engineering from the Nanjing University of Posts and Telecommunications, China, in 2007 and 2010, respectively. From 2012 to 2013, he was a Post-Doctoral Research Fellow with the Department of Electrical Engineering, Columbia University, USA. He is currently an Associate Professor with the College of Telecommunications and Information Engineering, Nanjing University of Posts and Telecommunications, China. His research interests include millimeter wave wireless communications, resource allocation in wireless networks, signal processing for communications, spectrum sensing for cognitive radio, and random matrix theory.

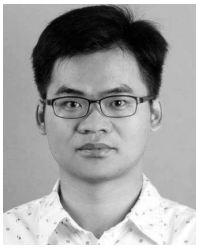

YULONG ZOU (SM'13) received the B.Eng. degree in information engineering from the Nanjing University of Posts and Telecommunications (NUPT), Nanjing, China, in 2006, the Ph.D. degree in electrical engineering from the Stevens Institute of Technology, Hoboken, NJ, USA, in 2012, and the Ph.D. degree in signal and information processing from NUPT, Nanjing, China, in 2012. He is currently a Professor and a Doctoral Supervisor with NUPT. His research interests span a wide range of topics in wireless communications and signal processing, including the cooperative communications, cognitive radio, wireless security, and energy-efficient communications. He acted as TPC members for the various IEEE sponsored conferences, e.g., IEEE ICC/GLOBECOM/WCNC/VTC/ICCC. He received the 9th IEEE Communications Society Asia-Pacific Best Young Researcher in 2014. He has been serving as an Editor for the IEEE COMMUNICATIONS SURVEYS AND TUTORIALS, *IET Communications*, and *China Communications*.